Brain Topography (2019) 32:445–460
https://doi.org/10.1007/s10548-018-0693-0

ORIGINAL PAPER

Spatially Overlapping Regions Show Abnormal Thalamo-frontal Circuit and Abnormal Precuneus in Disorders of Consciousness

Xiaoyan Wu[1] · Qiuyou Xie[2] · Xiaojin Liu[1] · Huiyuan Huang[1] · Qing Ma[2] · Junjing Wang[1] · Miao Zhong[1] · Yanbin He[2] · Chen Niu[1] · Yan Chen[2] · Feng Deng[1] · Xiaoxiao Ni[2] · Yuan He[1] · Yequn Guo[2] · Ronghao Yu[2] · Ruiwang Huang[1]

Received: 12 February 2018 / Accepted: 11 December 2018 / Published online: 1 February 2019

Abstract

Understanding the neural mechanisms of disorders of consciousness (DOC) is essential for estimating the conscious level and diagnosing DOC patients. Although previous studies reported brain functional connectivity (FC) and spontaneous neural activity patterns associated with consciousness, the relationship between them remains unclear. In this study, we identified the abnormal brain regions in DOC patients by performing voxel-wise FC strength (FCS) and fractional amplitude of low-frequency fluctuations (fALFF) analyses on resting-state functional magnetic resonance imaging data of 15 DOC patients and 24 healthy controls. Furthermore, we detected spatial intersections between two measures and estimated the correlations between either the FCS or the fALFF and the subscales of the Coma Recovery Scale-Revised (CRS-R). We found that the right superior frontal gyrus, left thalamus and right precuneus in which the DOC patients had a lower local FCS and fALFF than healthy controls, are coincident with regions of the mesocircuit model. In the right precuneus, the local FCS/fALFF was significantly positively correlated with the oromotor and motor scores/motor score of the CRS-R. Our findings may indicate that the co-occurrent pattern of spontaneous neural activity and functional connectivity in the thalamo-frontal circuit and the precuneus are associated with motor function in DOC patients.

Keywords Functional connectivity strength (FCS) · Fractional amplitude of low-frequency fluctuation (fALFF) · Co-occurrent pattern · Mesocircuit · Thalamo-frontal circuit · Precuneus

Introduction

Disorders of consciousness (DOC) include unresponsive wakefulness syndrome or vegetative state (UWS/VS) and minimally conscious state (MCS) (Owen 2008). Understanding the neural mechanisms of consciousness is important for estimating the conscious level and the possibility of consciousness recovery in DOC patients. Functional imaging is a valuable tool for understanding of consciousness. A number of imaging studies (Hannawi et al. 2015; Norton et al. 2012; Yao et al. 2015) reported abnormal crucial brain regions, such as the posterior cingulate cortex (PCC), precuneus, medial prefrontal cortex (mPFC), thalamus, and insula, all of which have been suggested as being associated with consciousness deficit in DOC patients. In contrast to identifying isolated brain region abnormalities, several studies indicated that abnormalities in the default mode network (DMN) (Amico et al. 2017; Boly et al. 2009; Rosazza et al. 2016; Vanhaudenhuyse et al. 2010) and in thalamo-cortical connectivity (Boly et al. 2009; Crone et al. 2016; Tang et al.

Communicated by Yun-Hee Kim.

Xiaoyan Wu and Qiuyou Xie contributed equally to this work.

Electronic supplementary material The online version of this article (https://doi.org/10.1007/s10548-018-0693-0) contains supplementary material, which is available to authorized users.

✉ Ronghao Yu
gesund@21cn.com

✉ Ruiwang Huang
ruiwang.huang@gmail.com

[1] Center for the Study of Applied Psychology, Guangdong Key Laboratory of Mental Health and Cognitive Science, School of Psychology, Institute for Brain Research and Rehabilitation, South China Normal University, Guangzhou 510631, People's Republic of China

[2] Coma Research Group, Center for Hyperbaric Oxygen and Neurorehabilitation, Guangzhou Hospital of Guangzhou Military Command, Guangzhou 510010, People's Republic of China

2011; Zhou et al. 2011) are related to the consciousness dysfunction in DOC patients. Most previous studies used only one type of measure, such as independent component analysis (ICA) (Norton et al. 2012; Vanhaudenhuyse et al. 2010), amplitude of low-frequency fluctuation (ALFF) (Yao et al. 2015), seed-based functional connectivity (FC) (Boly et al. 2009; Tang et al. 2011; Zhou et al. 2011), or network modeling to study brain function in DOC patients. In addition, the relationship between FC and brain spontaneous neural activity in DOC patients remains unclear.

In 2008, Schiff (2008) proposed the mesocircuit hypothesis to describe the processing of self and environmental information and to explain the vulnerable features of the anterior forebrain (frontal/prefrontal cortical-striatopallidal-thalamocortical loop systems) in DOC patients. Several studies also tested the mesocircuit model (Schiff 2010; Giacino et al. 2014). Monti et al. (2015) acquired functional magnetic resonance imaging (fMRI) data when DOC patients were performing a target detection task, selected the thalamus as a seed to calculate its functional connectivity to the prefrontal cortex, and revealed that impaired thalamo-frontal FC in DOC patients. Similarly, several other studies (Tang et al. 2011; Zhou et al. 2011) estimated thalamo-cortical FC in DOC patients by selecting the thalamus as a seed and calculating its FC with each voxel in the whole-brain using resting-state fMRI (R-fMRI). Zhou et al. (2011) showed lower specific (ventral and posterior of prefrontal and precuneus) and non-specific (dorsal prefrontal and anterior cingulate) thalamocortical FC in VS patients compared to healthy controls. However, Tang et al. (2011) found greater thalamocortical FC involving the frontal and temporal as well as cingulate regions, in mild traumatic brain injury (MTBI) patients compared to healthy controls. Although the above-mentioned fMRI research revealed disturbances in the mesocircuit that relate to consciousness deficits in DOC patients, most of them were seed-based FC studies based on a priori knowledge. Thus, the subjectivity of these studies may have biased the outcome and as a result may not have fully revealed the whole-brain FC.

Network models, which are constructed by taking each brain region as a node and the inter-nodal temporal correlation as an edge, have been used to analyze the topological properties of the whole-brain functional network in DOC patients (Achard et al. 2012; Liu et al. 2014; Maki-Marttunen et al. 2013). Recently, a voxel-wise whole-brain network approach (Sepulcre et al. 2010; Zuo et al. 2012; Kotchoubey et al. 2013) has been adopted to examine functional connectivity strength (FCS) in high spatial resolution brain networks. For a given voxel, the FCS measures the number of functional connections between the voxel and the rest of the voxels throughout the entire brain. To provide more spatial information of connectivity, Sepulcre et al. (2010) subdivided the FCS into the local and distant FCS based on the between-voxel Euclidean distance. The local and distant FCS, which quantify the spatial properties of FCS for a given voxel with other voxels inside or outside of predefined radius sphere, have been successfully applied in studies of various mental diseases (Beucke et al. 2013; Itahashi et al. 2015; Zhang et al. 2015) (see summarization in Table S1 in Supplementary Materials). In DOC patients, Wu et al. (2015) analyzed the FCS and distant FCS (outside 20 mm), and detected lower distant FCS primarily in regions belonging to the DMN, such as the PCC, precuneus, and MPFC, in patients compared to healthy controls. In addition, local FCS can be used to characterize the regional connectivity information of the brain (Itahashi et al. 2015). Thus in this study, we estimate local and distant connectivity to characterize spatial patterns of brain connectivity in the DOC patients.

In addition to the network model, several studies (He et al. 2014; Huang et al. 2014; Zhou et al. 2014) measured brain spontaneous neural activity in DOC patients by estimating the amplitude of low-frequency fluctuation (ALFF) or fractional ALFF (fALFF) (Zang et al. 2007; Zou et al. 2008) of R-fMRI data. ALFF represents the regional intensity of fluctuations in blood-oxygen-level-dependent (BOLD) signals, which are related to brain spontaneous neural activity and reflect the rate of firing of brain cortical neurons. Based on the rs-fMRI data, previous studies (Yao et al. 2015; He et al. 2014; Huang et al. 2014) found that the regions with lower ALFF are located in the thalamus and DMN (such as, precuneus, PCC, mPFC, and ACC), but the regions with higher ALFF were diverse or inconsistent, in DOC patients compared to healthy controls. Yao et al. (2015) reported higher ALFF in the insula, ACC, hippocampus, amygdala, and putamen in diffuse axonal injury patients compared to healthy controls. While He et al. (2014) showed higher ALFF in the insula, lingual gyrus, paracentral, and supplementary motor areas in DOC patients compared to healthy controls. The discrepancy of the brain regions with abnormal ALFF may be resulted from different lesion locations of DOC patients. Zhou et al. (2014) used a more sensitive and specific approach, fALFF (Zou et al. 2008), to estimate the spontaneous neural activity in MTBI patients and found significantly reduced fALFF in the thalamus, frontal, and temporal regions, which partially correspond to the mesocircuit.

Using a joint analysis based on multiple measures may provide a more sensitive approach for pinpointing the underlying mechanism responsible for consciousness in DOC patients. In fact, several studies (Itahashi et al. 2015; Mascali et al. 2015) also undertook a joint analysis, combining a network model with an ALFF (or fALFF) approach, to identify the abnormal brain regions and elucidate the relationship between brain FC and spontaneous neural activity in brain disorders. For example, Itahashi et al. (2015) combined local and distant FCS with fALFF to detect abnormal

brain regions in autism spectrum disorders. Mascali et al. (2015) studied the relationship between FC and ALFF and indicated that the FC had similar patterns to the ALFF in healthy controls, but the correlation patterns were disrupted in degenerative dementia patients. Huang et al. (2016) found a positive correlation between the standard deviation (SD) of the BOLD signal across time and FCS in healthy controls, but the correlation was absent in DOC patients. Huang et al. (2014) detected that both ALFF and FC were reduced in brain midline regions, including the perigenual anterior cingulate cortex (pACC), mPFC, and PCC in DOC patients compared to healthy controls. A multi-measures joint analysis may also reduce the effect of false positives and increase the reproducibility of the results (Blainey et al. 2014). To date, none of the studies we found combined local and distant FCS with a fALFF approach to analyze the relationship between FC and brain spontaneous neural activity in DOC patients.

In this study, we combined local and distant FCS with fALFF to identify the crucial brain regions associated with consciousness and to estimate the relationship between FC and brain spontaneous neural activity in DOC patients. First, we determined the brain regions with abnormal FCS and abnormal fALFF based on a voxel-wise analysis and then overlapped these abnormal regions in MNI space to detect the intersecting regions in the DOC patients. Finally, we estimated the correlations between the abnormal FCS and abnormal fALFF with the clinical performance of the DOC patients. Based on previous studies (Zhou et al. 2011, 2014; Monti et al. 2015; He et al. 2014; Huang et al. 2014), we hypothesis that the DOC patients may show altered spontaneous neural activity and also have impaired functional connectivity in the key area of mesocircuit such as, thalamus and frontal regions.

Materials and Methods

Subjects

Thirty-nine DOC patients were recruited from Guangzhou General Hospital of Guangzhou Military Command from May 2011 to March 2016. For each patient, the severity of their consciousness deficit was evaluated using the Coma Recovery Scale-Revised (CRS-R) (Giacino et al. 2004), which consists of six subscales - auditory, visual, motor, oromotor, communication, and arousal functions. To increase the reliability of the evaluation, 2–3 medical doctors assessed each patient together at the day before or after the scan. Utilizing the diagnostic criteria of the CRS-R, the patients were classified into UWS/VS and MCS. The UWS/VS patients showed arousal but no purposeful behaviors. The MCS patients included MCS- (visual pursuit, localization to noxious stimulation) and MCS+ (command following, no functional communication). The exclusion criteria for the DOC patients are shown in Fig. 1: (1) patients with metal implants or abnormal temperature; (2) patients younger than 18 years old (2 patients), older than 75 years old with obvious degradation of brain tissue (1 patient); (3) patients diagnosed with locked-in syndrome (LIS) and emergence from MCS (eMCS), showing functional communication (5 patients); and (4) excessive head motion (10 patients) or failure of spatial normalization (6 patients). The remaining fMRI data from 15 DOC patients (9 VS/6 MCS, 12M/3F, 41.40 ± 13.22 years old) were used for further analyses.

In addition, we recruited 24 age- and gender-matched healthy subjects (13 M/11 F, 34.92 ± 8.87 years old) as the controls. All subjects were right-handed and none had a history of neurological or psychiatric disorders. The patients did not take any antipsychotic and anesthetic medicine for 24 h before the scan. In this way, we could reduce the effect of medication on functional signal. The controls and the legal guardians of the patients signed informed consent forms prior to the study and they supported the publication of the manuscript. The study was approved by the Ethics Committee of Guangzhou General Hospital of Guangzhou Military Command, and all processes in accordance with the Declaration of Helsinki. Table 1 lists the detailed demographic and clinical information for the individual DOC patients. The composite demographic information for the subjects is listed in Table 2.

Data acquisition

All MRI data were obtained on a 3T GE MR scanner with an 8-channel phased-array head coil. The R-fMRI data were acquired using a single-shot gradient-echo echo-planar imaging (GE-EPI) sequence with the following parameters: repetition time (TR) = 2000 ms, echo time (TE) = 26 ms, flip angle (FA) = 90°, field of view (FoV) = 240×240 mm^2, data matrix = 64×64, slice thickness = 4.2 mm with inter-slice gap = 0.6 mm, voxel size = $3.75 \times 3.75 \times 4.2$ mm^3, 36 axial slices covering the whole brain, and 240 volumes obtained in 8 min. We also acquired high resolution brain structural images for each subject using a T1-weighted 3D fast Spoiled Gradient Recalled (FSPGR) sequence (TR = 8.864 ms, TE = 3.524 ms, FA = 13°, FoV = 240×240 mm^2, matrix = 256×256, slice thickness = 1 mm without an inter-slice gap, voxel size = $0.94 \times 0.94 \times 1$ mm^3, and 176 sagittal slices covering the whole brain). To reduce head movements, we stabilized each subject's head between two pieces of foam padding.

Fig. 1 Illustration of the exclusion criteria for the patients with disorders of consciousness (DOC). High resolution T1-weighted structural images are shown for the 39 DOC patients. We excluded 24 patients' datasets as they satisfied at least one of the following criteria, excessive head motion, younger than 18 years old, bad normalization or brain lesion or severe hydrocephalus, older than 75 years old, and diagnosed with LIS and EMCS

Data Preprocessing

All functional images were preprocessed using SPM12 (http://www.fil.ion.ucl.ac.uk/spm/software/) and the DPABI toolbox (Ver 2.0 http://rfmri.org/dpabi). For each subject, we removed the first 10 functional volumes to allow for adaptation to the environment and equilibrium of the MR signal and then performed slice-timing correction by taking the middle slice (18th) as the reference. Afterward, we performed a realignment to estimate head motion within the R-fMRI scan. The criteria for head motion were translation < 3 mm in any plane and rotation < 3° in any direction compared with the first time point. Thus, we excluded 10 patients' R-fMRI data due to their excessive head motion. The mean frame-wise displacement Jenkinson (FD-Jenkinson) (Jenkinson et al. 2002) was calculated for each subject. No significant difference in the mean FD-Jenkinson was found between the DOC patients and the healthy controls (Table 2).

To increase the accuracy of the segmentation and normalization for each subject, we reoriented those functional and structural images which were far away from the MNI space position. The next step was to co-register the brain structural images into functional space and then to segment the structural images into white matter (WM), gray matter (GM), and cerebrospinal fluid (CSF). Using the transformational matrix obtained in the segmentation step, we used all the subjects to create a group template using diffeomorphic anatomical registration through exponentiated lie algebra (DARTEL) (Ashburner 2007). Based on the group template, we normalized the functional images to standard MNI space with a resampled voxel size of $3 \times 3 \times 3$ mm^3.

Table 1 Demographic and clinical characteristics of the individual patients with disorders of consciousness (DOC) in this study

Patient	Gender	Age (years old)	Duration of DOC (days)	Lesion location	Diagnosis	Etiology	CRS-R scores	
							Au/V/M/O/C/Ar	Total
P01	M	39	25	Bilateral frontal, temporal, insula, basal ganglia and corpus callosum lesions	UWS/VS	HIE	0/0/2/1/0/2	5
P02	M	62	17	Right occipital lesion	UWS/VS	HIE	0/0/1/0/0/2	5
P03	M	48	32	Right occipital cortex hemorrhage, right upper epidural hemorrhage	UWS/VS	HIE	0/0/1/0/0/2	3
P04	M	21	69	Putamen, caudate, bilateral mastoid lesions	UWS/VS	HIE	1/0/2/1/0/1	5
P05	M	64	52	Bilateral frontal, temporal and parietal lesions	UWS/VS	TBI	0/0/1/1/0/2	4
P06	M	43	24	Bilateral frontal, temporal, insula, basal ganglia and corpus callosum lesions	UWS/VS	HIE	0/0/1/1/0/2	4
P07	M	41	42	Bilateral hippocampus, caudate lesions	MCS-	HIE	2/3/2/1/0/1	9
P08	F	20	63	Basal ganglia and left frontal lesions	MCS-	TBI	2/3/3/1/0/2	11
P09	M	32	287	Ventricle lesion	UWS/VS	HIE	1/0/1/1/0/2	5
P10	M	36	61	Bilateral frontal, parietal and occipital, precentral lesions	UWS/VS	HIE	1/0/0/0/0/1	2
P11	F	59	27	Diffused axonal injury, left frontotemporal and right occipital hemorrhage	MCS-	TBI	1/0/5/1/0/2	9
P12	F	46	68	Left frontal, temporal and parietal lesions	MCS-	TBI	1/0/3/1/0/2	7
P13	M	30	25	Diffused axonal injury, bilateral frontal, temporal and occipital, left parietal lesions	MCS-	TBI	1/1/3/2/0/2	9
P14	M	39	88	Diffused axonal injury	UWS/VS	TBI	0/0/2/1/0/2	5
P15	M	41	32	Right temporal and Corpus callosum lesions	MCS-	TBI	1/1/3/0/0/2	7

M, male; F, female; UWS/VS, unresponsive wakefulness syndrome /vegetative state; MCS, minimally conscious state, only MCS-(visual pursuit, localization to noxious stimulation) included in this study; HIE, hypoxic ischemic encephalopathy; TBI, traumatic brain injury; CRS-R, Coma Recovery Scale-Revised; Au, auditory; V, visual; M, motor; O, oromotor; C, communication; Ar, arousal

Table 2 Composite demographic data and head motions of the patients with disorders of consciousness (DOC) and the healthy controls (HC) in this study

	DOC	HC	Statistics	*p*-value
Demographic				
Gender (male/female)	12/3	13/11	$\chi^2 = 2.68$	0.10
Age (years old)	41.40 ± 13.22	34.92 ± 8.87	$t = 1.84$	0.07
Time prior to scan (day)	60.80 ± 66.06	N.A	N.A	N.A
Diagnosis (UWS or VS/MCS-)	9/6	N.A	N.A	N.A
Etiology (HIE/TBI)	8/7	N.A	N.A	N.A
Head motion				
Translation (mm)	0.11 ± 0.09	0.13 ± 0.08	$t = -0.67$	0.51
Rotation (radian)	0.20 ± 0.16	0.14 ± 0.11	$t = 1.41$	0.17
Mean FD Jenkinson	0.08 ± 0.08	0.07 ± 0.04	$t = 0.47$	0.65

UWS/VS, unresponsive wakefulness syndrome/vegetative state; MCS, minimally conscious state; HIE, hypoxic ischemic encephalopathy; TBI, traumatic brain injury; Mean FD Jenkinson, mean frame-wise displacement Jenkinson; N.A., non-applicable

To remove the noise signal, we detrended the data to eliminate linear trends and regressed out nuisances, including the WM and CSF in each voxel and 24 head motion profiles (6 head motion parameters, 6 head motion parameters one time point before, and the 12 corresponding squared items). To perform the regression, we used a component-based noise correction method (CompCor) (Behzadi et al. 2007) which identified the five principal components associated with physiological noise from GM and WM (or GM and CSF). We did not regress out the global signal, because doing so would alter the local and long-range correlations (Saad et al. 2012). Finally, before the voxel-wise local FCS and distant FCS, we bandpass filtered the signal between 0.01 and 0.1 Hz to reduce the effects of low-frequency drift and high-frequency physiological noise. Before calculating the fALFF, we performed spatial smoothing by using a 4 mm

FWHM Gaussian kernel to increase the signal-to-noise ratio (SNR). The flow chart shows the exact order of processing steps (see Fig. S1 in Supplementary Materials).

Local and Distant FCS

The FCS was computed using GRETNA (http://www.nitrc.org/projects/gretna/). For each subject, we constructed the voxel-wise whole-brain functional network by taking each voxel as a node and the inter-nodal Pearson's correlation coefficient (r) as the edge weight. First, we restricted the FC analysis to a pre-defined GM mask (GM tissue probability ≥ 20%, containing 67,541 voxels in MNI space) (Wu et al. 2015) to exclude artificial correlations from non-GM voxels. Then, we computed the weighted FCS for each voxel using the following equation (Buckner et al. 2009)

$$FCS_{\mathrm{i}} = \sum_{j=1}^{N} r_{ij} \quad (i \neq j), \tag{1}$$

where r_{ij} represents the correlation between any pair of voxels i and j and $N = 67{,}541$ is the number of voxels in the GM mask. Thus, we obtained a $67{,}541 \times 67{,}541$ matrix, the voxel-wise whole-brain connectivity matrix, for each subject by taking the inter-nodal correlation $r_{\mathrm{ij}} \geq 0.25$ as the threshold (Zhang et al. 2015a, b) (see Table S1 in Supplementary Materials). In this way, we may eliminate weak correlations that have arisen from noise (Zhang et al. 2015a, b).

To study the spatial information of the network topology, we defined two types of FCS, local FCS and distant FCS, by computing the FCS inside and outside of a 12 mm-radius sphere for a given voxel (Zhang et al. 2015a, b). Then, we separately converted the local FCS and distant FCS values to z-scores for each subject using the following equation

$$zFCS_i = \frac{FCS_{\mathrm{i}} - \mathrm{mean}(FCS)}{\sigma_{FCS}} \tag{2}$$

where mean(FCS) represents the mean FCS across all voxels in the GM mask and σ_{FCS} is the standard deviation of the FCS. Finally, we smoothed the zFCS maps with a 4-mm full-width at half maximum (FWHM) Gaussian kernel to generate szFCS maps for each subject (Zhang et al. 2015a, b).

Fractional ALFF

The fALFF value for each voxel was calculated using REST software (version V1.8) (http://restfmri.net/forum/index.php) to explore the brain spontaneous neural activity. We applied a Fast Fourier Transform (FFT) to transform the time series of each voxel into the frequency domain and computed the power spectrum for each voxel. The ratio of the square root of the power spectrum at a low-frequency range (0.01–0.1 Hz) to the entire frequency range (0-0.25 Hz) was calculated and was taken as the fALFF. The calculation was restricted within the pre-defined brain GM mask.

Statistical Analyses

A χ^2-test was used to test the statistical difference in gender between the DOC patients and the healthy controls. And a two-sample t-test was used to test between-group differences in age and head motions.

Two-sample t-tests were used to detect the differences in FCS or in fALFF between the DOC patients and the controls. In the calculations, we took age, gender, and the FD-Jenkinson as nuisance covariates. Additionally, we regressed out the brain GM signal to reduce the effect of brain atrophy. The significance level of the between-group difference was set at a threshold of $p < 0.05$ with a false discovery rate (FDR) correction. In this way, we determined the clusters showing significant between-group differences in local FCS, distant FCS, and fALFF.

For each of the clusters showing significant between-group differences, we examined the Spearman's correlations between FCS (or fALFF) values and the subscales of the CRS-R in the DOC patients. In the calculations, we also took age, gender, and the FD-Jenkinson as covariates and regressed them out.

Spatially Overlapping Regions

By overlapping all of the clusters determined from the local FCS, distant FCS, and fALFF in standard MNI space, we obtained the regions that intersected. To test the reliability of the overlapping approach and to provide a mean statistical significance, we performed a Monte Carlo simulation with 5,000 iterations (Itahashi et al. 2015). In each iteration step, we generated two Gaussian distribution brain maps within the pre-defined 20% GM mask based on the statistical mean and standard deviation of the t-maps of the FCS and fALFF. We first conducted a FDR correction ($p < 0.05$) for each of the two simulated maps and then overlapped the two maps in MNI space. Next, we determined the intersection regions and recorded the number of voxels within these regions. Finally, we compared the number of voxels in the actual intersection regions with those in the simulated data with a null distribution.

Correlations Between FCS (or fALFF) and Clinical Variables in the Intersection Regions

For each of the intersection regions, we estimated the Spearman's correlation between either the FCS or fALFF and each subscale of the CRS-R. In these calculations,

we also controlled for the effects of age, gender, and the FD-Jenkinson.

Robustness

To test the robustness of the above results, we repeated the voxel-wise analyses of the FCS using different analytical approaches, including using a binary network and choosing different r_{ij} thresholds. The overlap maps for the FCS and fALFF were constructed as described above. The local FCS and distant FCS were estimated separately. The validation of the local and distant FCS was implemented as follows.

Effect of Network Type on Local and Distant FCS

We repeated the network analyses by using the binary network for each subject. For a given node, we defined its local and distant FCS as the number of edges which were connected to other nodes ($r_{ij} \geq 0.25$) inside and outside of a 12 mm-radius sphere (see summarization in Table S1 in Supplementary Materials). After converting the voxel-wise local and distant FCS into z-scores, we obtained the zFCS map for each subject and then smoothed it using a 4 mm FWHM Gaussian kernel. Finally, we determined the clusters with significant between-group differences in the local or distant FCS (FDR corrected $p < 0.05$).

Effect of the r_{ij} Threshold on FCS

The choice of the r_{ij} threshold is controversial and arbitrary (Liu et al. 2015) when computing the FCS. Therefore, in addition to $r_{ij} \geq 0.25$, which was reported in the main text, we also computed the FCS using two other thresholds ($r_{ij} \geq 0.2$ and $r_{ij} \geq 0.3$) to test whether the FCS value depends on the selected threshold.

Effect of the Distance Length on FCS

Currently, we do not have a widely accepted standard for the distance selection for estimating the local and distant FCS. To test the robustness of our findings, we repeated the local and distant FCS calculation by setting a 20 mm-radius sphere.

Effect Size

To determine the reliability of statistic, we extracted local or distant FCS and fALFF value of the intersection regions, and estimated the effect size (Cohen d) according to Cohen's definition.

Results

Demographics and Head Motions of Subjects

The demographics and head motions of the subjects are listed in Table 2. No significant differences were found between the DOC patients and the controls for gender ($\chi^2 = 2.68$, $p = 0.10$), age ($t = 1.84$, $p = 0.07$), translation of head motion ($t = -0.67$, $p = 0.51$), rotation of head motion ($t = 1.41$, $p = 0.67$), and mean FD-Jenkinson ($t = 0.47$, $p = 0.65$).

Local and Distant FCS

Figure 2 shows the 13 clusters that showed significant between-group differences in local FCS. Five of the clusters showed a significantly greater local FCS, and eight clusters showed a significantly lower local FCS in the patients compared to the controls. The details about these 13 clusters are listed in Table 3. However, no cluster showed significant between-group difference in the distant FCS in the whole-brain. For each of the clusters shown in Fig. 2, the correlations between the local FCS and the subscales of the CRS-R in the DOC patients were listed in Table S2 (Supplementary materials).

Fractional ALFF

Figure 3 shows the 5 clusters with significant between-group differences in fALFF. Compared to the controls, the DOC patients had significantly increased fALFF in one cluster, which is located in the right cerebellum_crus2, but significantly decreased fALFF in four clusters, which are located in the right superior frontal gyrus (SFG), left middle frontal gyrus (MFG), left thalamus, and right precuneus. The details for these 5 clusters are listed in Table 4. For each of these 5 clusters, the correlations between fALFF and each subscale of the CRS-R were listed in Table S3 (Supplementary materials).

Spatially Overlapping Regions

Figure 4a illustrates the intersection regions obtained by overlapping all the clusters derived from both the local FCS and fALFF analyses into MNI space. In total, we obtained 3 intersection regions, which are located in the right SFG, left thalamus, and right precuneus. The scatter plot in Fig. 4b shows the local FCS against the fALFF across all the subjects in this study. The scatter plot makes it easy to see that the VS patients, MCS patients, and healthy controls had different distribution

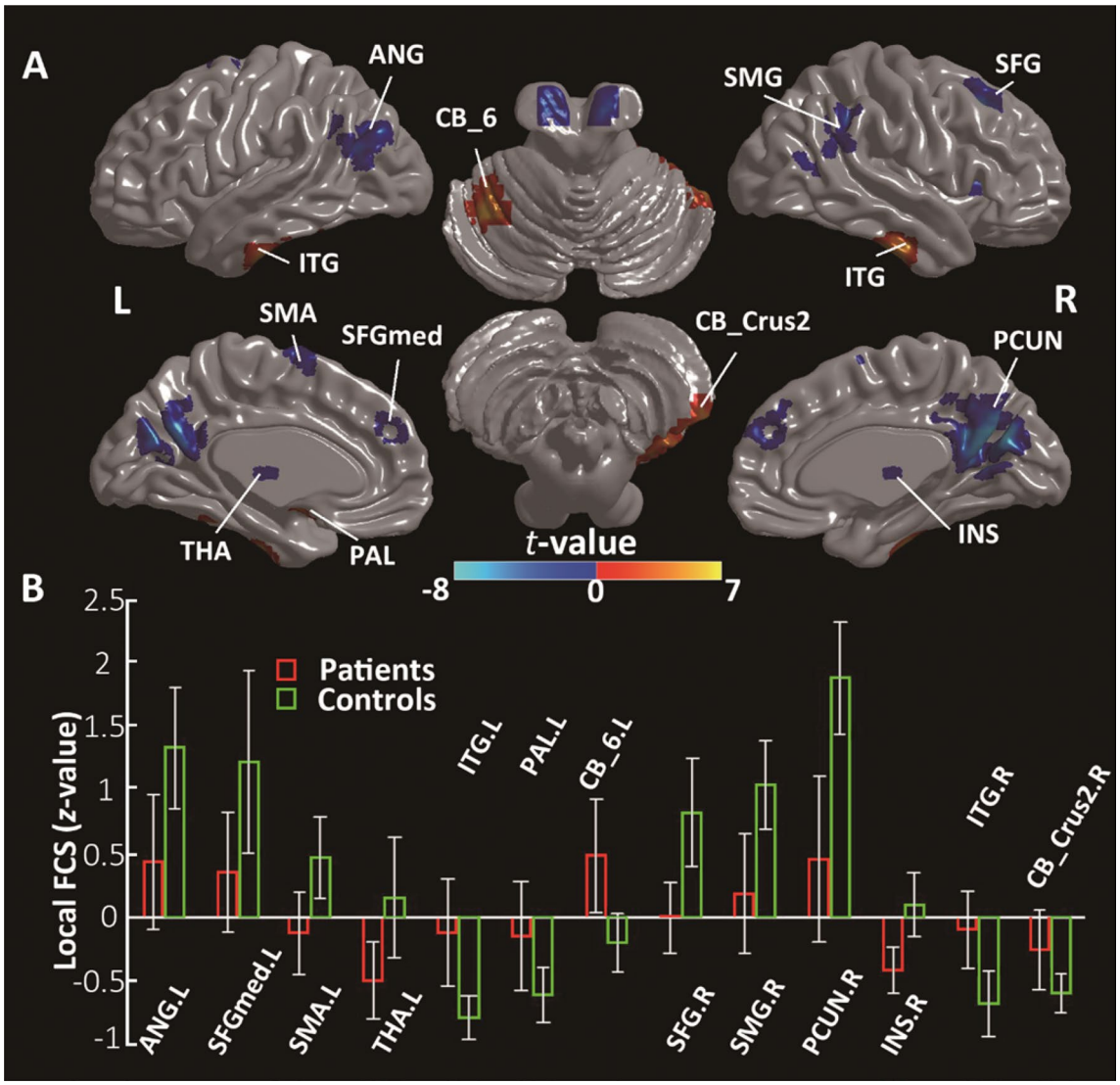

Fig. 2 Brain clusters with significant difference in the local functional connectivity strength (FCS) between the patients with disorders of consciousness (DOC) and the healthy controls ($p < 0.05$, FDR corrected). **a** Clusters location. The warmer (cooler) color indicates significantly increased (decreased) local FCS in the DOC patients compared to the controls. **b** Bar plot showing the local FCS value for each cluster. The bar height corresponds to the mean value and the error bar to the standard deviation. ANG, angular gyrus; SFGmed, medial superior frontal gyrus; SMA, supplementary motor area; THA, thalamus; ITG, inferior temporal gyrus; PAL, pallidum; CB_6, cerebelum_6; SFG, superior frontal gyrus; SMG, supramarginal gyrus; PCUN, precuneus; INS, insula; CB_Crus2, cerebelum_Crus2; L (R), left (right) hemisphere

patterns. Statistical analyses indicated that, for each of these 3 intersection regions, both the local FCS and fALFF were uniformly significantly decreased in the DOC patients compared to the controls. A Monte Carlo simulation analysis showed that the actual number of intersecting voxels (192 voxels) between these two measures was significantly higher than the number of intersecting voxels obtained using the simulation ($p < 0.0001$). The volume size of these 3 intersection regions was 45 voxels in the right SFG, 20 voxels in the left thalamus, and 102 voxels in the right precuneus.

Relationships Between FCS (or fALFF) and Clinical Variables in the Intersection Regions

For each of these three intersection regions (Fig. 4a), we calculated Spearman's correlations between the local FCS and each subscale of the CRS-R as well as between the fALFF and each subscale of the CRS-R in the DOC patients. The results are shown in Fig. 4c. The local FCS in the right precuneus was significantly positively correlated with the motor value of the CRS-R ($r = 0.68$, $p = 0.015$) and marginally significantly positively correlated with the oromotor value of

Table 3 Brain clusters showing significant difference in the local functional connectivity strength (FCS) between the patients with disorders of consciousness (DOC) and the healthy controls (HC) ($p < 0.05$, FDR-corrected). The clusters are reported according to the Anatomical Automatic Labeling (AAL-90) template with xjview8 (http://www.alivelearn.net/xjview/)

Index	Peak location	Cluster size (# Voxels)	Peak *t*-value	Peak coordinate in MNI space		
				x	*y*	*z*
Local FCS						
1	PCUN.R	535	−7.59	3	−69	24
2	SMG.R	112	−5.65	54	−45	27
3	SFG.R	60	−5.56	24	24	45
4	INS.R	143	−5.45	33	21	9
5	ANG.L	120	−4.82	−45	−63	25
6	THA.L	22	−4.56	−6	−12	3
7	SMA.L	26	−4.42	−9	3	63
8	SFGmed.L	49	−4.25	0	39	39
9	PAL.L	44	4.95	−18	0	−3
10	CB_Crus2.R	103	5.43	42	−39	−39
11	CB_6.L	46	5.67	−33	−54	−24
12	ITG.R	162	6.20	51	−15	−27
13	ITG.L	203	6.74	−48	−18	−33

PCUN, precuneus; SMG, supramarginal gyrus; SFG, superior frontal gyrus; INS, insula; ANG, angular gyrus; THA, thalamus; SMA, supplementary motor area; SFGmed, medial superior frontal gyrus; PAL, pallidum; CB_Crus2, cerebelum_Crus2; CB_6, cerebelum_6; ITG, inferior temporal gyrus; L (R), left (right) hemisphere

the CRS-R ($r = 0.57$, $p = 0.055$). We also detected that the fALFF in the right precuneus was marginally significantly positively correlated with the motor value of the CRS-R ($r = 0.57$, $p = 0.053$). More detailed correlation information is listed in Table S4 (Supplementary materials).

Robustness

We used both binary networks and different r_{ij} thresholds ($r_{ij} \geq 0.2/r_{ij} \geq 0.3$) to obtain the spatial distribution patterns that showed significant between-group differences in the local FCS. The results were basically in line with the main results (see Fig.S2 Supplementary materials). As expected, the intersection regions between the local FCS and fALFF were the same as those reported in the main text, that is, the intersection regions were still located in the right SFG, left thalamus, and right precuneus. Correlation analyses revealed that, for the right precuneus, either the local FCS or the fALFF was significantly positively correlated with the subscales of the CRS-R. In addition, we found that the DOC patients showed significant between-group differences in both local and distant FCS for setting a distance to 20 mm (see Table S5 in the Supplementary Materials). The intersection regions between the local FCS and fALFF are located in the thalamus and precuneus (see Fig. S2 in the Supplementary Materials), which is consistent with the main results corresponding to a 12 mm-radius sphere. For both the 12 mm-radius and 20 mm-radius spheres, we found that the local FCS and fALFF in the precuneus were significantly positively correlated with the subscales (motor value or oromotor value) of the CRS-R in the patients. However, the DOC patients showed not only altered distant FCS, but also an intersection region with co-reduced distant FCS and fALFF with a setting distance to 20 mm. Overall, statistical analyses reflected the robustness of main results even we selected different network types, r_{ij} thresholds, and distance length. The distance length selection may affect the determination of the altered distant FCS in the DOC patients.

Table S6 lists the effect size (Cohen *d*) of the local FCS and fALFF value in each intersection region. We found that effect sizes ranged from 0.6 to 0.8.

Discussion

This study examined patterns of connectivity and spontaneous neural activity in DOC patients by estimating the local FCS, distant FCS, and fALFF. We obtained the following results: (1) The local FCS was significantly increased in the cerebellum, bilateral inferior temporal gyrus (ITG), and left pallidum but decreased in the right insula, left thalamus, and association regions located in the frontal and parietal cortices (such as the right precuneus, right SMG, right SFG, left ANG, left SMA, and left SFGmed) in the patients compared to the healthy controls. (2) No significantly altered distant FCS was found in the patients compared to the controls. (3) The fALFF was significantly decreased in the left MFG, right SFG, left thalamus, and right precuneus. (4) For each of the intersection regions derived from the local FCS and fALFF analyses, we found uniformly significantly decreased

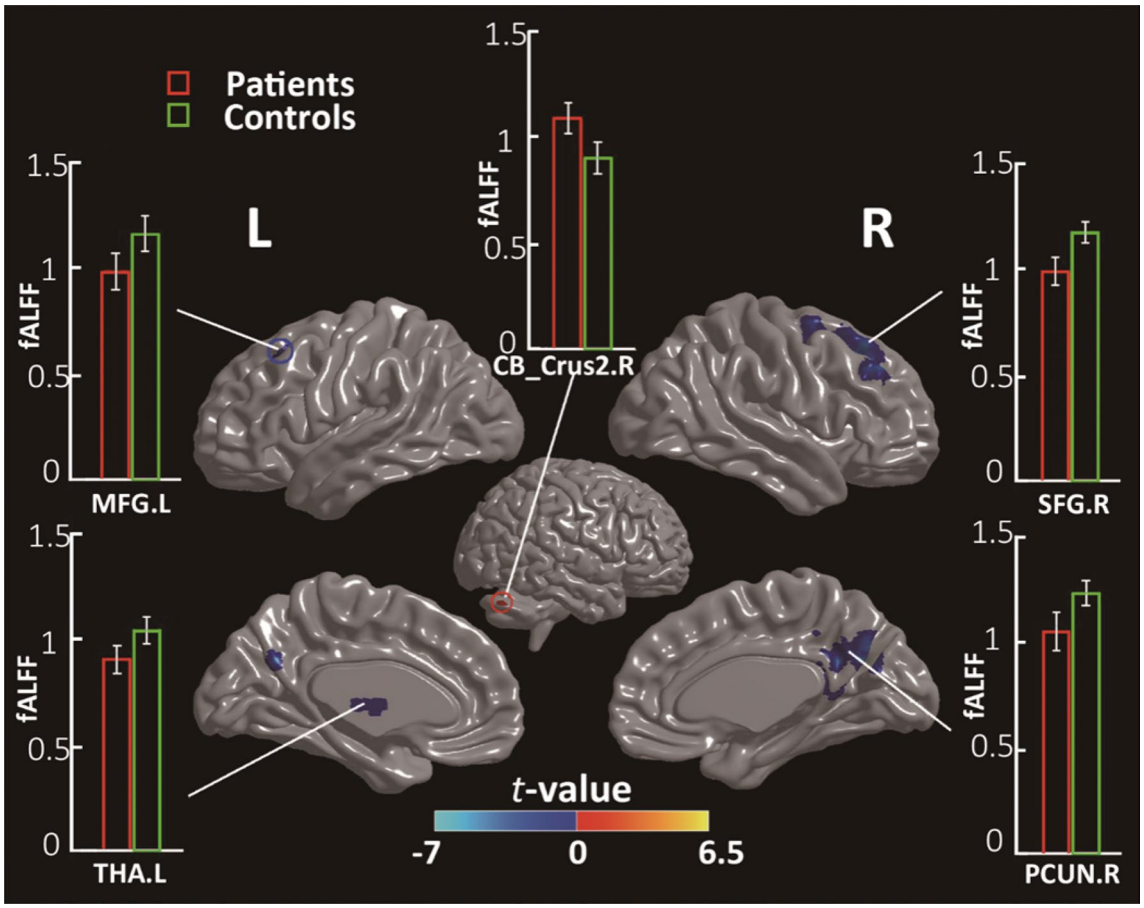

Fig. 3 Brain clusters with significant difference in the fractional amplitude of low-frequency fluctuations (fALFF) between the patients with disorders of consciousness (DOC) and the healthy controls ($p < 0.05$, FDR corrected). The warmer (cooler) color indicates significantly increased (decreased) fALFF in the DOC patients compared to the controls. The bar height corresponds to the mean value of the fALFF and the error bar to the standard deviation for a given group. MFG, middle frontal gyrus; THA, thalamus; CB_Crus2, cerebelum_Crus2; SFG, superior frontal gyrus; PCUN, precuneus; L (R), left (right) hemisphere

Table 4 Brain clusters showing significant differences in the fractional amplitude of low-frequency fluctuations (fALFF) between the patients with disorders of consciousness (DOC) and the healthy controls (HC) ($p < 0.05$, FDR-corrected)

Index	Peak location	Cluster size (#Voxels)	Peak *t*-value	Peak coordinate in MNI space		
				x	y	z
1	THA.L	32	−6.74	−6	−18	6
2	SFG.R	155	−6.73	21	24	48
3	PCUN.R	113	−6.35	3	−63	27
4	MFG.L	22	−5.99	−21	19	45
5	CB_Crus2.R	36	6.09	57	−57	−42

The brain clusters were reported according to the Anatomical Automatic Labeling (AAL-90) template with xjview8 (http://www.alivelearn.net/xjview/)

THA, thalamus; SFG, superior frontal gyrus; PCUN, precuneus; MFG, middle frontal gyrus; CB_Crus2, cerebelum_Crus2; L (R), left (right) hemisphere

local FCS and fALFF in the left thalamus, right SFG, and right precuneus. (5) A Spearman's correlation analysis revealed that the local FCS (fALFF) in the right precuneus was significantly positively correlated with the oromotor and motor scores (motor scores) of the CRS-R.

No Significantly Altered Distant FCS in DOC Patients

We found no significant difference in distant FCS between patients and controls, which is not consistency with previous studies (Boly et al. 2009; Tang et al. 2011; Zhou et al.

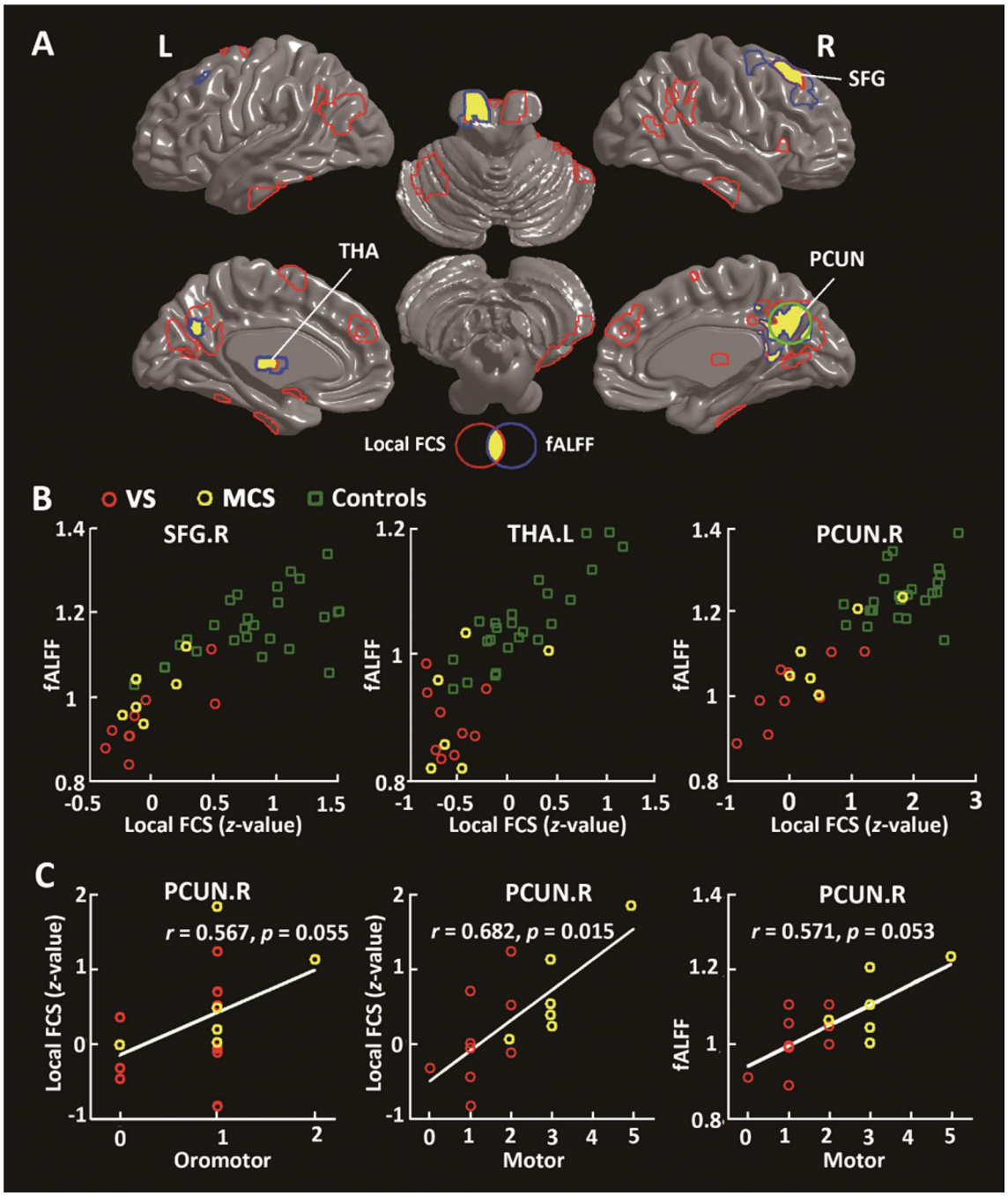

Fig. 4 Areas of intersection representing the shared abnormalities of both the local functional connectivity strength (FCS) and the fractional amplitude of low-frequency fluctuation (fALFF) in the patients with disorders of consciousness (DOC). **a** Intersection areas. The red (blue) contour indicates the clusters with significantly altered local FCS (fALFF). The yellow areas indicate the intersection regions. **b** Scatter plot of the fALFF against the local FCS for each intersection area. The symbol of "○" in red (yellow) stands for the VS (MCS) patients and the symbol of "□" in green for the healthy controls. **c** Correlations between the local FCS (or fALFF) and the identified subscales of the CRS-R ($p < 0.05$). SFG, superior frontal gyrus; THA, thalamus; PCUN, precuneus; L (R), left (right) hemispher

2011). This inconsistency may due to the different mathematic method for calculating distant connectivity or due to the radius of sphere which we select or due to sample difference. In the present study, we selected a 12 mm- radius sphere for a given voxel to perform data processing. While Wu et al. (2015) selected a 20 mm- radius sphere to estimate the distant FCS in DOC patients, and other studies of various mental diseases (Itahashi et al. 2015; Wang et al. 2014) used different radius (such as 25 mm or 75 mm) to compute distant FCS (see summarization in Table S1 in Supplementary

Materials). We also repeated the distant FCS by setting a 20 mm-radius sphere. We found the abnormal distant FCS in the cerebellum, fusiform gyrus, occipital cortices, and precuneus in the DOC patients compared to healthy controls. This further revealed that the different distance setting affects the detection of the altered distant FCS. In fact, the conventionally distant connectivity is computed as temporal signal correlations between seed region and voxels, or a pair of regions. Following previous studies (Beucke et al. 2013; Zhang et al. 2015a, b), we estimated the distant connectivity (distant FCS) as the sum of weighted connectivity outside of a 12 mm-radius sphere for a given voxel, which may mask out some altered specific connections due to altered connectivity with different directions or distance in DOC patients.

Higher Local FCS in DOC Patients

This study found that the DOC patients had greater local FCS in several regions, including the cerebellum, left pallidum, and bilateral ITG, compared to the healthy controls (Table 3; Fig. 2). The cerebellum has been suggested as being involved in a variety of functions, such as language, attention, motor, working memory, and delayed recall (Kansal 2017); the ITG participates in the higher levels of the ventral stream of visual processing and has been suggested to be associated with the representation of complex object features (Koivisto and Revonsuo 2010); and the pallidum participates in the mesocircuit of consciousness (Schiff 2010). In the mesocircuit model, the neurons of the pallidum actively inhibit the neurons of the central thalamus to reduce the connections between the thalamus and cortex (Crone et al. 2016; Giacino et al. 2014), resulting in consciousness deficits. Our results were consistent with several previous studies (Bisenius et al. 2015; Gooijers et al. 2016). Gooijers et al. (2016) conducted a bimanual tracking task in TBI patients and found enhanced activation in the left cerebellum crus2 in patients compared to healthy subjects during the execution phase. Tacikowski et al. (2017) detected brain activity connected with self-related information in healthy controls and found that the ITG was involved in unaware processing of self-related information. Bisenius et al. (2015) performed a meta-analysis of 19 fMRI studies and found that the ITG was a crucial region for visual consciousness. In this study, we also found that the increased local FCS in this left ITG was negatively correlated with the visual subscore of the CRS-R in the DOC patients (see Table S2 Supplementary materials). These findings may indicate that great deficits in visual consciousness occur in DOC patients.

Lower Local FCS and fALFF in the DOC Patients

This study found that both the local FCS (Table 3; Fig. 2) and the fALFF (Table 4; Fig. 3) were lower in regions of the frontal, parietal, and subcortical cortices in the DOC patients compared to the controls. The finding of lower local FCS and fALFF in the frontal and parietal regions is consistent with several previous studies (Boly et al. 2011; Quentin et al. 2014) in DOC patients. Boly et al. (2011) used event-related potentials (ERP) to measure effective connectivity during auditory processing in DOC patients and found impaired effectivity connectivity from the frontal to the temporal lobes in the VS patients compared to the healthy controls. Based on brain structural MRI data, Quentin et al. (2014) found that a WM connection between the frontal and parietal cortices was related to visual perception consciousness. In an auditory consciousness study, Brancucci et al. (2016) found that the frontal cortices, rather than the parietal cortices, participated in auditory consciousness processing. Koch et al. (2016) suggested that the crucial regions related to consciousness may be located in the posterior cortical hot zone rather than the frontal and parietal cortices. Thus, the types of stimuli may be key influences when investigating the neural correlates of consciousness (Quentin et al. 2014; Brancucci et al. 2016). In the present study, we found decreased local FCS in subcortical regions, including the left thalamus and right insula, in the DOC patients. The insula is believed to participate in the processing of interoceptive information, which relates to bodily self-consciousness, with exteroceptive information (52). Brancucci et al. (2016) also showed that the insula is a crucial node for auditory consciousness. Thus, an impaired insula may cause deficits in processing internal and external information in DOC patients. In this study, we also found that the fALFF was lower in the left thalamus of the DOC patients, a finding which is in line with previous studies (Yao et al. 2015). Yao et al. (2015) analyzed the ALFF in diffuse axonal injury patients and found decreased ALFF in the thalamus in the patients compared to healthy controls. Zhou et al. (2014) analyzed the fALFF in MTBI patients and also found lower fALFF in the thalamus of the patients compared to healthy controls. Our finding of lower fALFF in the thalamus may indicate disrupted regional spontaneous neural activity of the thalamus in the DOC patients.

Spatial Intersection Regions in the Thalamo-frontal Circuit and Precuneus

Co-occurred reductions of local FCS and abnormal fALFF were detected in the DOC patients in 3 common regions, the right SFG, left thalamus, and right precuneus (Fig. 4a). Interestingly, these 3 regions are coincident with those of a previous network study, in which van den Heuvel et al. (Heuvel and Sporns 2011) constructed human brain structural networks in healthy subjects based on diffusion tensor imaging (DTI) data and detected hub regions located in the SFG, precuneus, and thalamus. Our finding of these three

regions implies that these hubs play key roles in patients with impaired consciousness and appears to partly corroborate the mesocircuit hypothesis, which was proposed by Schiff (2010).

This study found disrupted local FCS and fALFF in the right SFG (prefrontal cortex) and left thalamus (Fig. 4a). The abnormal morphology and function of thalamus have been reported to relate to consciousness. Lutkenhoff et al. (2015) analyzed T1-weighted high resolution brain structural data and reported GM atrophy in the thalamus of DOC patients. Fernández-Espejo et al. (2011) analyzed DTI data and found decreased mean diffusivity (MD) in the thalamus in VS patients compared to MCS patients. Gili et al. (2013) analyzed the properties of brain functional networks in healthy subjects under propofol anesthesia and found decreased centrality in the thalamus of mildly sedated subjects compared to awake ones. Crone et al. (2014)analyzed the properties of brain functional networks in chronic DOC patients and found these patients had a decreased degree in the thalamus. Furthermore, the thalamus is involved in relaying sensory and motor signals to the cerebral cortex, and the human brain produces consciousness by the thalamus integrating internal experience and external information from multiple neural areas and transmitting the integrated information into the cerebral association area (Laureys et al. 2015). These may indicate that impairment of the thalamus reduces its ability to integrate information and is related to the deficit of consciousness in DOC patients. In addition, Monti et al. (2015) suggested disrupted thalamo-frontal circuit in DOC patients. Lant et al. (2016) detected structural disconnection between the thalamus and the medial frontal cortex in DOC patients. Taken together, our finding of decreased local FCS and fALFF in the thalamus and SFG indicated that the disrupted thalamo-fontal connectivity, may lead to impaired consciousness in DOC patients.

The precuneus, a key region in the DMN, has been suggested as being involved in self and environmental information processing, and as being associated with self-related mental representations such as self-referential thought and mind wandering (Cavanna and Trimble 2006). This study revealed that both the local FCS and the fALFF in the right precuneus were significantly positively correlated with the CRS-R value (Fig. 4c), which is used to evaluate the consciousness level or the severity of impaired consciousness in DOC patients. Our findings of abnormal FCS and fALFF in the precuneus are in line with several previous studies (Hannawi et al. 2015; Vanhaudenhuyse et al. 2010) that reported decreased spontaneous neural activity or intrinsic FC in the DMN in DOC patients. Qiu et al. (2017) combined multi-model analysis FC and cerebral blood flow (CBF) and showed lower connectivity in the DMN and lower CBF in the DMN, frontoparietal network, and thalamus. Thus, our findings of decreased local FCS and fALFF in the SFG, thalamus, and precuneus may indicate disruptions of local organization and activity in the precuneus and the thalamo-frontal circuit in DOC patients.

It is remarkable that we detected the common regions with abnormal local FCS and fALFF in precuneus, right SFG, and thalamus in the DOC patients. Additional analysis for each group showed a co-activity pattern between local FCS (or distant FCS) and fALFF in DMN, which are located in right precuneus, left angular, right supramarginal, and right SFG (right precuneus), in the healthy controls, but no co-activity region was found in the DOC patients. This result is partly in line with several previous studies. Mascali et al. (2015) found that healthy subjects had positive correlation between FC and ALFF in the DMN (ACC, PCC), suggesting that the greater functional connectivity is associated with greater spontaneous neural activity. Huang et al. (2014) also found lower ALFF and FC in pACC, mPFC, PCC in DOC patients compared to healthy controls. By combining PET and rs-fMRI, Riedl et al. (2014) indicated that intrinsic connectivity was determined by spontaneous neural activity in healthy subjects. Di et al. (2013) found that functional connectivity in several regions, including the ACC, mPFC, precuneus, basal ganglia and thalamus, was related to ALFF in old male DOC patients. Actually, it is hard to infer the casual relationship between the reduced spontaneous neural activity and local functional connectivity in the thalamo-frontal circuit and precuneus in the patients. Our findings of the synchronous reductions in these two local functional measures indicated the disruptions of local function in these three regions (thalamus, SFG and precuneus), which may be related to clinical performance (such as motor and oromotor) in DOC patients.

Limitations

Several limitation factors in the present study need to be addressed here. First, the small sample size (15 DOC patients, including 9 VS and 6 MCS-) may bias the generality of our results. Actually, we recruited 39 DOC patients, only 15 of them met the inclusion criteria since images distortion, or bad normalization, or brain lesion and severe hydrocephalus. In this study, we used two different measures, FCS and fALFF, to analyze the fMRI data and found the intersected regions showing both abnormal local FCS and abnormal fALFF in MNI space in the DOC patients. Using this multi-modal analyses may reduce the likelihood of obtaining false positives findings, improve the specificity or repeatability of the results, and lessen the impact of the limited sample size. We noticed that it is still controversial for choosing large or small sample size to obtain the reliable result. Friston (2012, 2013) suggested that the optimum experimental design should sensitize inference to large effect size but not based on the sample size, and mentioned that

the suitable sample sizes is on the order of 16 to 32 for a neuroimaging study. Desmond and Glover (2002) suggested that the effect size is more important than the significant difference. In this study, we estimated the effect size to show the reliability of significance when we observed significant difference between the DOC patients and healthy controls. Second, the excessive head movement in the DOC patients could have affected the realignment and caused poor normalization, which would reduce the comparability between the patients and the healthy controls. To reduce the head motion effect, we excluded the functional datasets of 10 patients with head motion exclusion criteria, which were translation < 3 mm in any plane and rotation < 3° in any direction. We also matched the translation, rotation, and FD_Jenkinson between the patients and the healthy controls and controlled for the FD_Jenkinson in the statistical analysis. To promote normalization, we performed a normalization using DARTEL, a high-dimensional image registration approach, which is believed to be a useful algorithm for diffeomorphic image registration (Ashburner 2007). Even so, it was still difficult to get well normalized functional images for the DOC patients due to brain injury and severe brain atrophy. Thus, we excluded the functional datasets of 6 patients with poor normalization from further analysis. Third, we did not sub-classify the DOC patients into different subgroups, such as HIE and TBI patients or VS/UWS and MCS patients, according to their pathogenesis or diagnosis. This may reduce the clinical applicability of our findings. In fact, the small sample size is the reason we put all the DOC patients into a single group to compare with the controls. Future studies will need to recruit more DOC patients so that they can be sub-classified into different subgroups according to their pathogenesis or diagnosis. In this way, we can explore the abnormal brain spontaneous neural activity and connectivity in patients with different levels of consciousness to provide more information regarding the neuronal correlates of consciousness. In addition, the DOC patients showed heterogeneous lesion locations in the brain. The calculations of functional connectivity and its relationship with the clinical symptom of consciousness may be affected by the lesion location. In the calculation, we applied a strict inclusion criteria to exclude the DOC patients with the bad normalization, brain lesion, and severe hydrocephalus (Fig. 1) (Weng et al. 2017). For the heterogeneous lesion locations, a further study with large sample of DOC patients is needed to detect the effect of the lesion location on functional connectivity and consciousness in DOC patients. Fourth, we only performed CRS-R assessment at the day before or after the scan without considering the variability of the response. Cortese et al. (2015) showed that the CRS-R score varies with assess time in DOC patients. Thus, multiple CRS-R testing may be helpful for reducing misdiagnosis. In this study, each patient was not assessed CRS-R score repeatedly, but was assessed by 2–3 medical doctors to make the evaluation relatively reliable. Fifth, the option arrangement of processing step is diverse, such as spatial smoothing Gaussian kernel size (4 mm, or 6 mm, or 8 mm FWHM), threshold of r_{ij} (0.2, or 0.25, or 0.3), distance of radius sphere (12 mm or 20 mm), and network type (weighted or binary). There is no specific and standard option arrangement for analyzing fMRI data and we are limited our ability to perform all of these arrangements. In practice, we have tested the effect of different thresholds of r_{ij}, network types, and distance length, on the FCS. Statistical analyses showed the robustness of the main results even though the selection of distance length affected the distant FCS. Actually, a previous study (Zhu et al. 2017) about patients with major depressive disorder (MDD) also found that FCS abnormalities are dependent on distance length in MDD. In the future, we may need to set multiple different thresholds of the distance length to estimate FCS for detecting the abnormality of FCS in DOC patients. Finally, this study used a cross-sectional resting-state fMRI design to explain the abnormal brain spontaneous neural activity, so it cannot provide key brain regions that relate to changes and developments in the consciousness levels of DOC patients. Further longitudinal studies are needed to study the development of consciousness in a single DOC patient group as well as between different groups.

In summary, we studied brain intrinsic connectivity and spontaneous neural activity by computing the FCS and fALFF separately in DOC patients. Uniformly, the DOC patients showed decreased local FCS and fALFF in the SFG, thalamus, and precuneus compared to healthy controls. These co-occurrent reductions indicate local functional disruption of thalamo-frontal circuit and precuneus in DOC patients. Our findings provided additional evidence to support the mesocircuit model (particularly thalamo-frontal circuit) and suggested that hub regions, such as the precuneus, are crucial for understanding the underlying neural basis of DOC patients.

Acknowledgements This work was supported by funding from the National Natural Science Foundation of China (Grant Numbers: 81871338, 81371535, 81428013, 81471654, 81271548, and 81871338), Natural Science Foundation of Guangdong Province, China (2015A030313609). The authors express their appreciation to Drs. Rhoda E. and Edmund F. Perozzi for editing assistance.

Author contributions XW analysed the data, wrote the manuscript, and revised the manuscript. XL, HH assisted the data analysis and the manuscript revision. JW, MZ, CN, FD, YH participated in discussion, give some advices for details of the manuscript. QX, RY, QM collected the MRI data and clinical information. YH, YC, XN, YG, assisted to collect the clinical information. RH is the guider of the manuscript, provide the idea of the manuscript and advice of revision.

Compliance with Ethical Standards

Conflict of interest The authors declare that they have no competing financial interests.

References

Achard S et al (2012) Hubs of brain functional networks are radically reorganized in comatose patients. Proc Natl Acad Sci USA 109(50):20608–20613

Amico E et al (2017) Mapping the functional connectome traits of levels of consciousness. Neuroimage 148:201–211

Ashburner J (2007) A fast diffeomorphic image registration algorithm. Neuroimage 38(1):95–113

Behzadi Y et al (2007) A component based noise correction method (CompCor) for BOLD and perfusion based fMRI. Neuroimage 37(1):90–101

Beucke JC et al (2013) Abnormally high degree connectivity of the orbitofrontal cortex in obsessive-compulsive disorder. JAMA Psychiatry 70(6):619–629

Bisenius S et al (2015) Identifying neural correlates of visual consciousness with ALE meta-analyses. Neuroimage 122:177–187

Blainey P, Krzywinski M, Altman N (2014) Points of significance: replication. Nat Methods 11(9):879–880

Boly M et al (2009) Functional connectivity in the default network during resting state is preserved in a vegetative but not in a brain dead patient. Hum Brain Mapp 30(8):2393–2400

Boly M et al (2011) Preserved feedforward but impaired top-down processes in the vegetative state. Science 332(6031):858–862

Brancucci A et al (2016) A frontal but not parietal neural correlate of auditory consciousness. Brain Struct Funct 221(1):463–472

Buckner RL et al (2009) Cortical hubs revealed by intrinsic functional connectivity: mapping, assessment of stability, and relation to Alzheimer's disease. J Neurosci 29(6):1860–1873

Cavanna AE, Trimble MR (2006) The precuneus: a review of its functional anatomy and behavioural correlates. Brain 129(Pt 3):564–583

Cortese MD et al (2015) Coma recovery scale-r: variability in the disorder of consciousness. BMC Neurol 15:186

Craig AD (2009) How do you feel—now? the anterior insula and human awareness. Nat Rev Neurosci 10(1): 59

Crone JS et al (2014) Altered network properties of the fronto-parietal network and the thalamus in impaired consciousness. Neuroimage Clin 4:240–248

Crone JS et al (2016) Testing proposed neuronal models of effective connectivity within the cortico-basal Ganglia-thalamo-cortical loop during loss of consciousness. Cereb Cortex 27(4):2727–2738

Desmond JE, Glover GH (2002) Eatimating sample size in functional MRI (fMRI) neuroimaging studies: statistical power analyses. J Neurosci Method 118(2002):115–128

Di X et al (2013) The influence of the amplitude of low-frequency fluctuations on resting-state functional connectivity. Front Hum Neurosci 7:118

Fernández-Espejo D et al (2011) Diffusion weighted imaging distinguishes the vegetative state from the minimally conscious state. Neuroimage 54(1):103–112

Friston K (2012) Ten ironic rules for non-statistical reviewers. Neuroimage 61(4):1300–1310

Friston K (2013) Sample size and the fallacies of classical inference. Neuroimage 81:503–504

Giacino JT, Kalmar K, Whyte J (2004) The JFK Coma Recovery Scale-Revised: Measurement characteristics and diagnostic utility. Arch Phys Med Rehabil 85(12):2020–2029

Giacino JT et al (2014) Disorders of consciousness after acquired brain injury: the state of the science. Nat Rev Neurol 10(2):99–114

Gili T et al (2013) The thalamus and brainstem act as key hubs in alterations of human brain network connectivity induced by mild propofol sedation. J Neurosci 33(9):4024–4031

Gooijers J et al (2016) Movement preparation and execution: differential functional activation patterns after traumatic brain injury. Brain 139(Pt 9):2469–2485

Hannawi Y et al (2015) Resting brain activity in disorders of consciousness A systematic review and meta-analysis. Neurology 84(12):1272–1280

He JH et al (2014) Hyperactive external awareness against hypoactive internal awareness in disorders of consciousness using resting-state functional MRI: highlighting the involvement of visuo-motor modulation. NMR Biomed 27(8):880–886

Huang Z et al (2014) The self and its resting state in consciousness: an investigation of the vegetative state. Hum Brain Mapp 35(5):1997–2008

Huang Z et al (2016) Decoupled temporal variability and signal synchronization of spontaneous brain activity in loss of consciousness: An fMRI study in anesthesia. Neuroimage 124:693–703

Itahashi T et al (2015) Alterations of local spontaneous brain activity and connectivity in adults with high-functioning autism spectrum disorder. Mol Autism 6:30

Jenkinson M et al (2002) Improved optimization for the robust and accurate linear registration and motion correction of brain images. Neuroimage 17(2):825–841

Kansal K et al.(2017) Structural cerebellar correlates of cognitive and motor dysfunctions in cerebellar degeneration. Brain 140:707–720

Koch C et al (2016) Neural correlates of consciousness: progress and problems. Nat Rev Neurosci 17(5):307–321

Koivisto M, Revonsuo A (2010) Event-related brain potential correlates of visual awareness. Neurosci Biobehav Rev 34(6):922–934

Kotchoubey B et al (2013) Global functional connectivity reveals highly significant differences between the vegetative and the minimally conscious state. Journal of neurology 260(4):975–983

Lant ND et al (2016) Relationship between the anterior forebrain mesocircuit and the default mode network in the structural bases of disorders of consciousness. Neuroimage Clin 10:27–35

Laureys S, Gosseries O, Tononi G (2015) The neurology of consciousness: cognitive neuroscience and neuropathology. Academic Press, New York

Liu X et al (2014) Scale-free functional connectivity of the brain is maintained in anesthetized healthy participants but not in patients with unresponsive wakefulness syndrome. PLoS ONE 9(3):e92182

Liu W et al (2015) Abnormal degree centrality of functional hubs associated with negative coping in older Chinese adults who lost their only child. Biol Psychol 112:46–55

Lutkenhoff ES et al (2015) Thalamic and extrathalamic mechanisms of consciousness after severe brain injury. Ann Neurol 78(1):68–76

Maki-Marttunen Vn et al (2013) Disruption of transfer entropy and inter-hemispheric brain functional connectivity in patients with disorder of consciousness. Front Neuroinform 14(Suppl 1):P83

Mascali D et al (2015) Intrinsic patterns of coupling between correlation and amplitude of low-frequency fMRI fluctuations are disrupted in degenerative dementia mainly due to functional disconnection. PLoS ONE 10(4):e0120988

Monti MM et al (2015) Thalamo-frontal connectivity mediates top-down cognitive functions in disorders of consciousness. Neurology 84(2):167–173

Norton L et al (2012) Disruptions of functional connectivity in the default mode network of comatose patients. Neurology 78(3):175–181

Owen AM (2008) Disorders of consciousness. Ann N Y Acad Sci 1124:225–38

Qiu M et al (2017) Multi-modal analysis of functional connectivity and cerebral blood flow reveals shared and unique effects of propofol in large-scale brain networks. Neuroimage 148:130–140

Quentin R et al (2014) Fronto-parietal anatomical connections influence the modulation of conscious visual perception by high-beta frontal oscillatory activity. Cereb Cortex 25(8):2095–2101

Riedl V et al (2014) Local activity determines functional connectivity in the resting human brain: a simultaneous FDG-PET/fMRI study. J Neurosci 34:6260–6266

Rosazza C et al (2016) Multimodal study of default-mode network integrity in disorders of consciousness. Ann Neurol 79(5):841–853

Saad ZS et al (2012) Trouble at rest: how correlation patterns and group differences become distorted after global signal regression. Brain Connect 2(1):25–32

Schiff ND (2008) Central thalamic contributions to arousal regulation and neurological disorders of consciousness. Ann N Y Acad Sci 1129:105–118

Schiff ND (2010) Recovery of consciousness after brain injury: a mesocircuit hypothesis. Trends Neurosci 33(1):1–9

Sepulcre J et al (2010) The organization of local and distant functional connectivity in the human brain. PLoS Comput Biol 6(6):e1000808

Tacikowski P, Berger CC, Ehrsson HH (2017) Dissociating the neural basis of conceptual self-awareness from perceptual awareness and unaware self-processing. Cereb Cortex 27(7):3768–3781

Tang L et al (2011) Thalamic resting-state functional networks: disruption in patients with mild traumatic brain injury. Radiology 260(3):831–840

van den Heuvel MP, Sporns O (2011) Rich-club organization of the human connectome. J Neurosci 31(44):15775–15786

Vanhaudenhuyse A et al (2010) Default network connectivity reflects the level of consciousness in non-communicative brain-damaged patients. Brain 133(1):161–171

Wang T et al (2014) Abnormal functional connectivity density in children with anisometropic amblyopia at resting-state. Brain Res 1563:41–51

Weng L et al (2017) Abnormal structural connectivity between the basal ganglia, thalamus, and frontal cortex in patients with disorders of consciousness. Cortex 90:71–87

Wu X et al (2015) Intrinsic Functional Connectivity Patterns Predict Consciousness Level and Recovery Outcome in Acquired Brain Injury. J Neurosci 35(37):12932–12946

Yao S et al (2015) Thalamocortical Sensorimotor Circuit Damage Associated with Disorders of Consciousness for Diffuse Axonal Injury Patients. J Neurol Sci 356(1):168–174

Zang YF et al (2007) Altered baseline brain activity in children with ADHD revealed by resting-state functional MRI. Brain Dev 29(2):83–91

Zhang X-D et al (2015a) Long- and short-range functional connectivity density alteration in non-alcoholic cirrhotic patients one month after liver transplantation: A resting-state fMRI study. Brain Res 1620:177–187

Zhang J et al (2015b) Abnormal functional connectivity density in Parkinson's disease. Behav Brain Res 280:113–118

Zhou J et al (2011) Specific and nonspecific thalamocortical functional connectivity in normal and vegetative states. Conscious Cogn 20(2):257–268

Zhou Y et al (2014) Characterization of Thalamo-cortical Association Using Amplitude and Connectivity of Functional MRI in Mild Traumatic Brain Injury. J Magn Reson Imaging 39:1558–1568

Zhu J et al (2017) Distance-dependent alterations in local functional connectivity in drug-naive major depressive disorder. Psychiatry Res Neuroimaging 270:80–85

Zou Q et al (2008) An improved approach to detection of amplitude of low-frequency fluctuation (ALFF) for resting-state fMRI: fractional ALFF. J Neurosci Methods 172(1):137–141

Zuo XN et al (2012) Network centrality in the human functional connectome. Cereb Cortex 22(8):1862–1875